JOURNAL OF
NEUROPHYSIOLOGY

January 1989
Volume 61, Number 1

(Continued)

IMPORTANT CHANGE

As of July 1, 1989, the reference style for the *Journal of Neurophysiology* is changing in text from serial numbering to author's name and date. The unnumbered reference list should continue to be arranged alphabetically by author. See Information for Contributors for details and examples. It will be appreciated if authors of manuscripts submitted under the old system can make these changes during revision.

JOURNAL OF
NEUROPHYSIOLOGY

February 1989
Volume 61, Number 2

(Continued)

IMPORTANT CHANGE

As of July 1, 1989, the reference style for the *Journal of Neurophysiology* is changing in text from serial numbering to author's name and date. The unnumbered reference list should continue to be arranged alphabetically by author. See Information for Contributors for details and examples. It will be appreciated if authors of manuscripts submitted under the old system can make these changes during revision.

JOURNAL OF
NEUROPHYSIOLOGY

March 1989
Volume 61, Number 3

(Continued)

IMPORTANT CHANGE

As of July 1, 1989, the reference style for the *Journal of Neurophysiology* is changing in text from serial numbering to author's name and date. The unnumbered reference list should continue to be arranged alphabetically by author. See Information for Contributors for details and examples. It will be appreciated if authors of manuscripts submitted under the old system can make these changes during revision.

JOURNAL OF NEUROPHYSIOLOGY
Vol. 61, No. 3, March 1989. *Printed in U.S.A.*

EPSPs in Rat Neocortical Neurons in Vitro
I. Electrophysiological Evidence for Two Distinct EPSPs

BERND SUTOR AND JOHN J. HABLITZ
Section of Neurophysiology, Department of Neurology, Baylor College of Medicine, Houston, Texas 77030

SUMMARY AND CONCLUSIONS

1. To investigate excitatory postsynaptic potentials (EPSPs), intracellular recordings were performed in layer II/III neurons of the rat medial frontal cortex. The average resting membrane potential of the neurons was more than −75 mV and their average input resistance was >20 MΩ. The amplitudes of the action potentials evoked by injection of depolarizing current pulses were >100 mV. The electrophysiological properties of the neurons recorded were similar to those of regular-spiking pyramidal cells.

2. Current-voltage relationships, determined by injecting inward and outward current pulses, displayed considerable inward rectification in both the depolarizing and hyperpolarizing directions. The steady-state input resistance increased with depolarization and decreased with hyperpolarization, concomitant with increases and decreases, respectively, in the membrane time constant.

3. Postsynaptic potentials were evoked by electrical stimulation via a bipolar electrode positioned in layer IV of the neocortex. Stimulus-response relationships, determined by gradually increasing the stimulus intensity, were consistent among the population of neurons examined. A short-latency EPSP [early EPSP (eEPSP)] was the response with the lowest threshold. Amplitudes of the eEPSP ranged from 4 to 8 mV. Following a hyperpolarization of the membrane potential, the amplitude of the eEPSP decreased. Upon depolarization, a slight increase in amplitude and duration was observed, accompanied by a significant increase in time to peak.

4. The membrane current underlying the eEPSP (eEPSC) was measured using the single-electrode voltage-clamp method. The amplitude of the eEPSC was apparently independent of the membrane potential in 8 of 12 neurons tested. In the other 4 neurons, the amplitude of the eEPSC increased with hyperpolarization and decreased with depolarization.

5. Higher stimulus intensities evoked, in addition to the eEPSP, a delayed EPSP [late EPSP (lEPSP)] in >90% of the neurons tested. The amplitude of the lEPSP ranged from 12 to 20 mV, and the latency varied between 20 and 60 ms. The amplitude of the lEPSP varied with membrane potential, decreasing with depolarization and increasing following hyperpolarization. The membrane current underlying the lEPSP (lEPSC) displayed a similar voltage dependence.

6. At stimulus intensities that led to the activation of inhibitory postsynaptic potentials (IPSPs), the lEPSP was no longer observed. This is attributed to a shunting effect of the large conductance increase associated with IPSPs.

7. In contrast to the eEPSP, the lEPSP was not able to follow stimulus frequencies > 0.5 Hz, suggesting that a polysynaptic pathway is involved in the generation of the lEPSP.

8. High-frequency stimulation (HFS) resulted in a selective and sustained increase in the amplitude of the lEPSP. This change resembled that seen during long-term potentiation (LTP) in hippocampal neurons. The effects of HFS could be observed only at stimulus intensities below the activation threshold for IPSPs, suggesting that significant LTP in neocortical neurons can be induced in the presence of intact inhibitory synaptic mechanisms.

9. These experiments provide evidence for the existence of two electrophysiologically distinct EPSPs in neocortical neurons. We suggest that the eEPSP is generated at synapses remote from the soma and that its shape at different membrane potentials is largely determined by the nonlinear properties of the somatic membrane. The lEPSP is polysynaptic in nature and probably originates from synapses located on, or close to, the soma.

INTRODUCTION

Soon after the first intracellular recordings were made from mammalian neocortical neurons in vivo (33), investigations of the excitatory and inhibitory inputs to these cells demonstrated the complex nature of excitatory postsynaptic potentials (EPSPs) elicited by stimulation of afferent pathways (1, 20–22, 27, 31, 35, 36, 42, 43, 49, 51). The time course and latency of the EPSPs were found to depend on the afferent pathway activated. Following electrical stimulation of specific thalamic nuclei, nonspecific thalamic nuclei, and the mesencephalic reticular formation, respectively, three different types of EPSPs, which differed with respect to time course and synaptic efficacy, were observed in neurons of the cat motor cortex (20). Antidromic activation of the pyramidal tract elicited recurrent EPSPs in pyramidal tract cells, suggesting a mutual excitatory interaction between these neurons (1, 19, 42, 49). A characteristic feature of recurrent EPSPs was a slight reduction in their amplitudes when the membrane potential was hyperpolarized (49). In contrast, the amplitudes of the EPSPs evoked by thalamic or transcallosal stimulation were apparently independent of the membrane potential (31, 49). The differences in the properties of the EPSPs elicited by stimulation of certain pathways were attributed to differences in the location of the corresponding synapses, i.e., close to or remote from the soma (20, 31, 42, 49), or differences in the responsiveness of the subsynaptic membrane (20), or both.

In addition to the variability of neocortical EPSPs evoked by stimulation of different pathways, it was shown that these postsynaptic potentials display frequency-dependent, dynamic changes following repetitive activation of a single afferent pathway. Upon repetitive stimulation of specific or nonspecific thalamic nuclei, an augmenting or recruiting response, respectively, could be recorded from the cortical surface (10, 11). Intracellular recordings re-

vealed significant changes in the EPSP amplitude and duration (20, 22, 35, 36). The augmenting response, evoked by repetitive stimulation of the nucleus ventralis lateralis, was associated with the appearance of a delayed second EPSP (22).

Another form of frequency-dependent changes in neocortical EPSPs recorded in vivo was first described by Baranyi and Feher (3) and Bindman et al. (6). High-frequency stimulation (HFS) of afferent pathways led to a sustained increase in excitatory synaptic transmission in neocortical neurons. In more recent studies, this long-term potentiation (LTP) was described in greater detail using in vivo (4, 23) and in vitro (2, 7, 23–25) experimental models.

Because afferent pathways are interrupted during the preparation of neocortical brain slices, the investigation of EPSPs in such slices would seem to be limited. It has been possible, however, to examine local excitatory pathways in the neocortex (53). EPSPs recorded in neocortical neurons in vitro have been described by several groups. Connors et al. (9) reported that two different EPSPs could be evoked by electrical stimulation of the pial surface. Following activation of callosal fibers, Vogt and Gorman (53) observed several types of EPSPs in layer V neurons of the cingulate cortex that differed in their time course, amplitude, and ability to produce action potentials. In a more detailed study, Thomson (50) described an EPSP in rat neocortical neurons whose properties resembled those of *N*-methyl-D-aspartate (NMDA) on neocortical neurons.

The in vitro studies described above either focused on the description of stimulus-response patterns or investigated EPSP pharmacology. The influence of nonlinear membrane properties on postsynaptic potentials was not considered. The marked stability of intracellular recordings in vitro and the ability to influence the neuron's microenvironment provide excellent experimental conditions for the correlated study of the biophysical and pharmacological properties of EPSPs in neocortical neurons. In the present series of papers, we describe the electrophysiological and pharmacological characteristics of EPSPs recorded in layer II/III neurons of the rat frontal cortex following activation of a synaptic connection that should remain intact in a slice preparation, namely, local projections from cortical layer IV. This paper provides evidence for two distinct EPSPs evoked by electrical stimulation with different intensities and describes the electrophysiological properties of these EPSPs. A second paper (47) investigates some of the pharmacological characteristics of the EPSPs, especially the involvement of NMDA receptors in their mediation. In addition, it presents experiments studying the effects of changes in extracellular magnesium concentration on membrane properties and EPSPs. Parts of these investigations have been published previously in abstract form (45, 46).

METHODS

Preparation and solutions

The techniques employed to prepare brain slices from rat frontal cortex have been described previously (48). Briefly, male Sprague-Dawley rats (120–160 g) were anesthetized with ether and decapitated. The brains were quickly removed and stored in ice-cold saline for 30 s to 1 min. Slices with a nominal thickness of 500 μm were prepared using a McIlwain tissue chopper. Six slices were typically obtained from each hemisphere and stored in saline at room temperature. Following a preincubation period of at least 1 h, 4–6 slices were transferred to an interface-type chamber. Saline was continuously perfused from below at a flow rate of about 1 ml/min. Over another period of 1 h, the chamber was slowly warmed to the recording temperature of 34–35°C.

The saline consisted of the following (in mM): 125 NaCl, 3.5 KCl, 1.25 NaH_2PO_4, 2.5 $CaCl_2$, 1.3 $MgSO_4$, 25 $NaHCO_3$, and 10 glucose. The solution was continuously perfused with a mixture of 95% O_2 and 5% CO_2 to attain a steady-state oxygenation level and to maintain a pH value of 7.4.

Recording techniques

Intracellular recordings were obtained from superficially located cortical neurons by means of glass microelectrodes. The pipettes were pulled from thick-walled, filament-containing, borosilicate glass tubings (1.5 mm OD) and filled with 4 M potassium acetate (KAc, adjusted to pH 7.2 with acetic acid). The resistance of these electrodes ranged from 50 to 90 MΩ.

Intracellular signals were recorded and amplified using an npi SEC 1L single-electrode current- and voltage-clamp amplifier (npi, Tamm, FRG). This device allowed intracellular current injection via either a bridge circuit or a time-sharing system (switched current-clamp) that consisted of a high-frequency alternation between potential measurement and current injection. When using the switched current-clamp mode, the output signal of the head-stage amplifier was continuously monitored on a separate oscilloscope. At low switching frequencies (6–10 kHz), the voltage transients during current passage were adjusted, using capacitance compensation, to obtain a rectangular form. The switching frequency was then set to the maximum value that still permitted complete decay of each voltage transient prior to the next voltage sample. Due to an improved design of the capacitance neutralization circuit (34), it was possible, with the electrodes employed, to use switching frequencies between 18 and 21 kHz at a duty cycle of 25%. All current-clamp recordings presented in this study were performed using the switched current-clamp mode of the amplifier. The adjustment of the amplifier's voltage-clamp mode and the criteria for the selection of microelectrodes with properties necessary to perform single-electrode voltage-clamp measurements were as described previously (48).

Figure 1 compares the performance of the amplifier in voltage-clamp mode during an intracellular recording (Fig. 1*A*) and when connected to a "neuron model" (Fig. 1*B*). In both cases, the holding potential was adjusted to the "zero current line" (−80 mV in Fig. 1*A* and 0 mV in Fig. 1*B*), and depolarizing and hyperpolarizing voltage steps of 30-mV amplitude were applied. The settling time for the step change of the neuron's membrane potential as well as for the voltage step produced at the "neuron model" was <1 ms. There was no difference between the time course and amplitude of the voltage steps. However, the capacitive transients of the membrane currents recorded in the neuron were quite different from those of the currents observed with the "neuron model." Using the "neuron model," the capacitive transients were short (<1 ms) and symmetrical. After the replacement of the resistance that represented the electrode by a glass microelectrode filled with 4 M KAc (60 MΩ), no significant changes in the capacitive transients were observed, indicating that the amplifier's capacitance neutralization was capable of effectively compensating for the microelectrode's capacity. The capacitive transients associated with the neuronal membrane current lasted 10–20 ms and were asymmetrical. The reason for these differences were twofold.

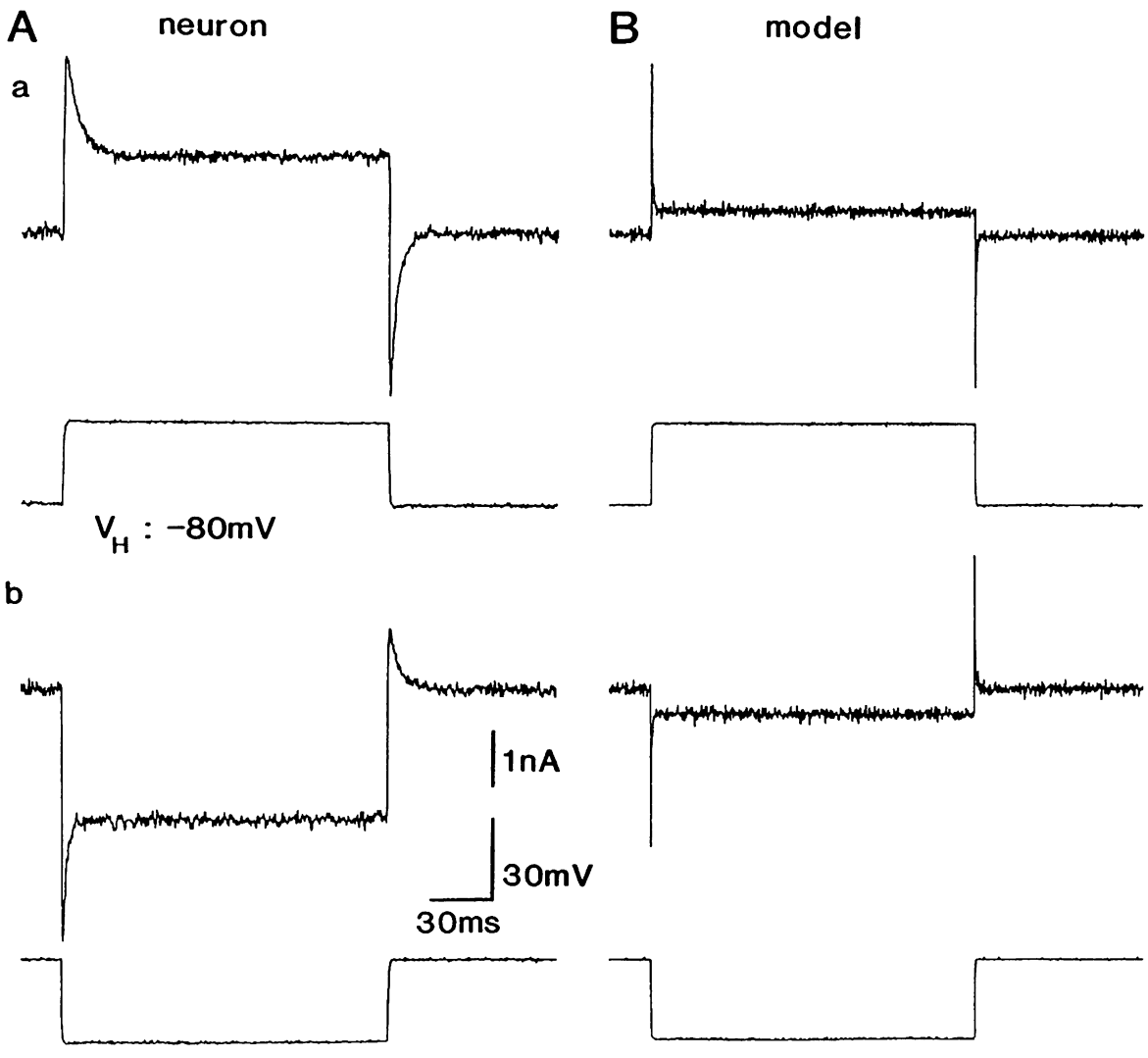

FIG. 1. Comparison of single-electrode voltage-clamp recordings performed in a neocortical neuron (*A*) and using a "neuron model" (*B*). *A*: membrane potential of the neuron was clamped to its RMP (holding potential [V_H] = −80 mV = RMP), and depolarizing (*a*) and hyperpolarizing (*b*) voltage steps (30 mV, 150 ms) were applied. The traces shown are averages of 3 measurements. In this and all other voltage-clamp figures, the *upper trace* of each panel represents the current and the *lower trace* the voltage. *B*: an experiment similar to that depicted in *A* was performed using a "neuron model" consisting of an RC circuit with a 50 MΩ resistor and a 50-pF capacitor connected in series to a 70 MΩ resistance representing the microelectrode. The measurements were carried out at the zero current line of the head-stage output signal. Five single sweeps were averaged. In *A* and *B*, the switching frequency of the amplifier was 19.5 kHz at a duty cycle of 25%. The membrane currents were filtered at 1 (*A*) and 2 kHz (*B*), respectively.

First, activation and inactivation of voltage-dependent currents contribute to the recordings in the neuron. Second, it is most likely that there was an imperfect "space clamp" of the neuron, despite a good voltage clamp of the membrane potential of that area of neuronal membrane that could be effectively controlled by the microelectrode (probably the somatic membrane or parts of it). Part of the longer capacitive transient is due to the charging of remote membrane. It is important to note that insufficient space-clamp conditions, inherent in voltage-clamp measurements in neuronal elements with an extensive dendritic arborization (37), also affect current-clamp measurements, i.e., the determination of the voltage dependence or reversal potential of an EPSP that is generated at sites located on distal dendrites (18). The present studies were designed to assess relative changes in two synaptic potentials recorded simultaneously in the same neuron. Differential effects of changes in membrane potential on one potential or the other allow inferences to be made about mechanisms of generation of the somatically recorded response, even though space-clamp conditions are not ideal.

Stimulation

Postsynaptic potentials were elicited by means of bipolar stimulation electrodes (platinum-iridium wire 30 μm diam) positioned in cortical layer IV (as judged by the distance below the pial surface), ~0.5–1.0 mm from the recording electrode. Such stimulation should principally activate local projections from layer IV although excitation of fibers of passage cannot be ruled out. The stimulus strength was set by changing the stimulus duration. At a stimulus duration of 20 μs, the current necessary to evoke an eEPSP was determined, and then the stimulus duration was increased in steps of 10–20 μs using a digital timer (WPI 1800 series stimulator). This method allowed an accurate and reproducible determination of stimulus-response relationships. Comparisons

with measurements in which the stimulus current instead of the stimulus duration was changed revealed no differences in the response pattern. In this study, stimulus intensities are given either as the charge applied to the electrode (in nanocoulombs) or as multiples of the threshold intensity (T) necessary for synaptically evoking an action potential.

Data acquisition and analysis

The recorded signals were displayed on a storage oscilloscope and stored on videotape following digitization using a Neuro-Corder DR 384 (frequency response DC 22 kHz for each channel). For subsequent analysis, the signals were replayed and digitized by means of a laboratory computer (PDP $11/23^{+}$) using digitizing rates between 122 and 1,220 μs per point. The plots and diagrams were made on a digital plotter (HP 7470A). During the experiments, a Brush Instruments Mark 200 chart recorder was employed for continuous monitoring of the membrane potential.

All values are given as means ± SD. Statistical comparisons of mean values were performed using the Student's *t* test.

RESULTS

Electrophysiological properties of rat neocortical neurons

Intracellular recordings were obtained from 74 neurons located in layer II/III of the rat medial precentral cortex. The resting membrane potential (RMP) of these neurons was −79.3 ± 4.6 (SD) mV. The input resistance (R_N) of the neurons was determined either by injecting a hyperpolarizing current pulse (150 ms, 0.3–0.5 nA) and measuring the corresponding voltage deviation at the end of the pulse or by calculating the slope of the current-voltage (*I-V*) curve (see Fig. 2*B*) at the intercept of the coordinate axes. The mean value of R_N was 21.6 ± 4.3 (SD) MΩ. Upon injection of depolarizing current pulses, neurons responded, at threshold, with an action potential (Fig. 2*C*) whose mean amplitude was 104.8 ± 8.9 mV. Injection of outward current pulses with suprathreshold intensities evoked repetitive discharges of action potentials (Fig. 2*C*). On the basis of these electrophysiological data, the neurons recorded can be classified as regular spiking cells (29, 48, 54).

I-V curves were obtained to examine the possibility that nonlinear membrane properties may exist in cortical neurons and contribute to voltage-dependent changes in synaptic responses. In agreement with a previous study (48), the *I-V* curves of rat neocortical neurons were found to be nonlinear over the entire range of membrane potentials investigated (RMP ± 40 mV). The neurons displayed time-dependent and time-independent inward rectification in both the hyperpolarizing and depolarizing directions

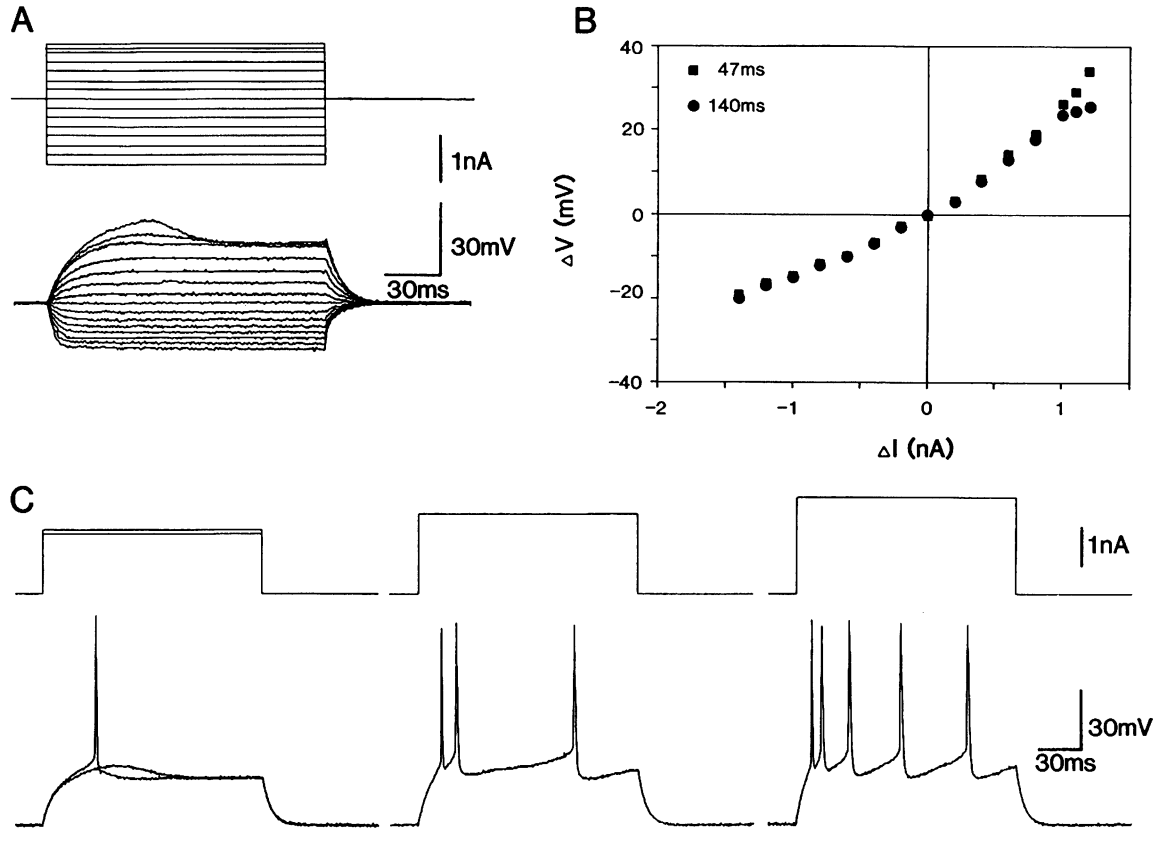

FIG. 2. Current-voltage relationship and discharge behavior of rat neocortical neurons. *A*: specimen records showing response to hyperpolarizing and subthreshold depolarizing current pulses of variable amplitude (pulse duration, 150 ms). The consecutively performed measurements were superimposed (RMP, −82 mV). *B*: plot of the voltage amplitudes measured at 47 ms (*squares*) and 140 ms (*circles*) after the onset of the current pulse as a function of the current amplitudes injected (same cell as in *A*). The resulting *I-V* curve depicts depolarizing and hyperpolarizing inward rectification. Note the time-dependent difference in the *I-V* curves at membrane potentials 20 mV positive to the RMP. *C*: responses of another neuron (RMP, −85 mV) to threshold (*left*, 1.6 nA) and suprathreshold (*center*, 2.0, and *right*, 2.4 nA) depolarizing current pulses (150 ms). The *left panel* shows, in addition, the neuronal response to a just subthreshold current pulse (1.5 nA).

(Fig. 2, *A* and *B*). To quantify the magnitude of the overall inward rectification, a rectification ratio was calculated from the quotient of the R_N determined at a membrane potential of -55 ± 2 mV and the R_N measured at a membrane potential of -80 ± 2 mV (9). The mean value of the rectification ratio was found to be 1.77 ± 0.39 (SD; $n = 15$), i.e., the R_N at membrane potentials close to the firing threshold was almost twice as large as at membrane potentials close to the RMP. This is also shown in Fig. 3. In this neuron, the R_N was determined at different membrane potentials by injecting hyperpolarizing current pulses and measuring the corresponding voltage deviations (Fig. 3*A*). The plot of the R_N as a function of the membrane potential clearly illustrates that, with regard to the RMP, the R_N increased with depolarization and decreased with hyperpolarization (Fig. 3*B*). In addition, when the membrane time constant was analyzed at different membrane potentials by fitting a single exponential function to the charging curves, using a least-squares method, the membrane time constant increased with depolarization and decreased with hyperpolarization relative to the RMP (Fig. 3*B*). On the assumption of a more or less constant first equalizing time constant (37), the estimated electrotonic length constant would also increase with depolarization, i.e., the neuron would become electrotonically more compact at membrane potentials close to the firing level. Such changes could be expected to influence both the amplitude and time course of synaptic potentials.

Stimulus-response characteristics of neocortical neurons

Figure 4*A* shows synaptic potentials evoked in a neocortical neuron by stimuli of varying intensities applied to layer IV. At very low intensities (4.5 nC), a small EPSP was elicited. In a given neuron, the latency of this EPSP was short (2–5 ms), constant, and independent of the membrane potential. When the membrane potential was depolarized by 10–20 mV and measurements were made of R_N at different times after the stimulus, there was no evidence of an inhibitory postsynaptic potential (IPSP). Because of its short latency, this EPSP was termed the early EPSP (eEPSP). The eEPSP was always the first measurable synaptic response evoked by low-intensity stimulation (see also Fig. 5, *A* and *B*, and Fig. 11). In the population of neurons studied ($n = 20$), the eEPSP had an amplitude of 6.6 ± 2.3 mV, a time to peak of 8.6 ± 4.2 (SD) ms, and a duration of 47.6 ± 18.2 ms.

Increasing the stimulus strength to 13.5 nC produced, following the eEPSP, a delayed, slowly rising depolarizing potential (Fig. 4*A*) with all the characteristic features of an EPSP (see below). At stimulus intensities at threshold for this response, the late EPSP (lEPSP) had an amplitude of 16.3 ± 4.2 mV ($n = 15$), a time to peak of 40.1 ± 11.4 ms, and a duration of 130.1 ± 26.1 ms. In a given neuron, at RMP and with a constant stimulus intensity, the lEPSP displayed a quite variable latency ranging from 10 to 40 ms. A further increase in stimulus intensity led first to a substantial decrease in the latency (Fig. 4*A*, 22.5 nC) and then to the disappearance of the lEPSP. At a stimulus strength sufficient to evoke an action potential (i.e., 1 T) (Fig. 4*A*, 55 nC), there was no detectable lEPSP. This paradoxical behavior can be attributed to a shunt of the lEPSP by chloride- and potassium-dependent IPSPs elicited at higher stimulation strengths (Fig. 4*C*, *left*). As described previously for neocortical neurons (9, 15, 16, 44, 54), at RMP, the chloride-dependent IPSPs appeared as depolarizing potentials (Fig. 4*C*, 1.5 T, *left*) associated with a 70–90% decrease in R_N. Upon depolarization of the membrane potential to values positive to -70 mV, the polarity of the IPSP reversed (Fig. 4*C*, *right*). The equilibrium potential of the chloride-dependent IPSP (E_{IPSP}) was -70.9 ± 4.4 mV ($n = 10$). This value is similar to those reported in earlier studies (15, 16). Following reversal of the chloride-dependent IPSP, a potassium-dependent late IPSP (lIPSP) also became obvious (Fig. 4*C*, *right*). Due to the relatively

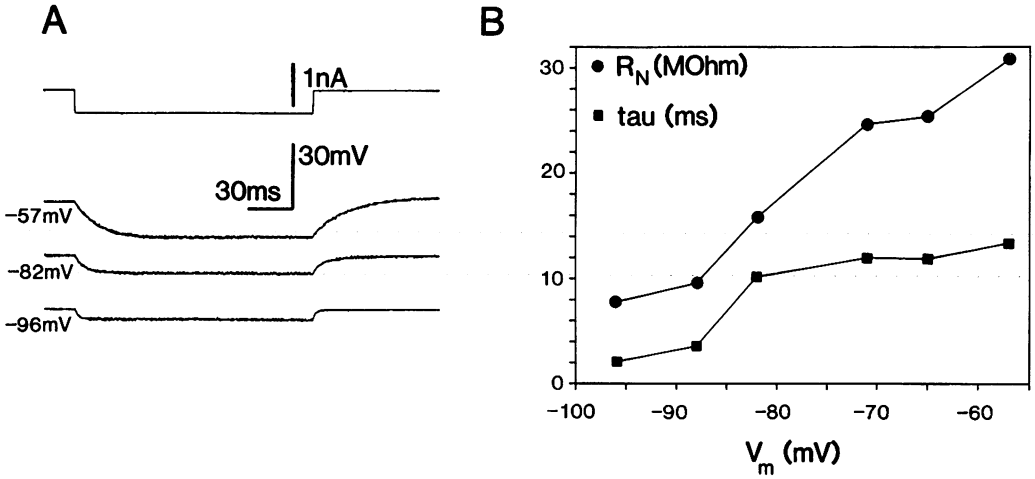

FIG. 3. Relationship between input resistance (R_N), time constant (tau), and membrane potential. *A*: determination of R_N at different membrane potentials by injecting hyperpolarizing current pulses (0.5 nA, 150 ms) and measuring the corresponding voltage deviation 145 ms after the onset of the current pulse (RMP, −82 mV). The membrane potential was changed by direct current pulses of 1-s duration with intervals of 5–10 s between the individual measurements. *B*: plot of R_N (*circles*) (as derived from measurements described in *A*) and of tau (*squares*) as a function of membrane potential. The time constant was determined by fitting a single exponential function to the voltage transient following the offset of the current pulse.

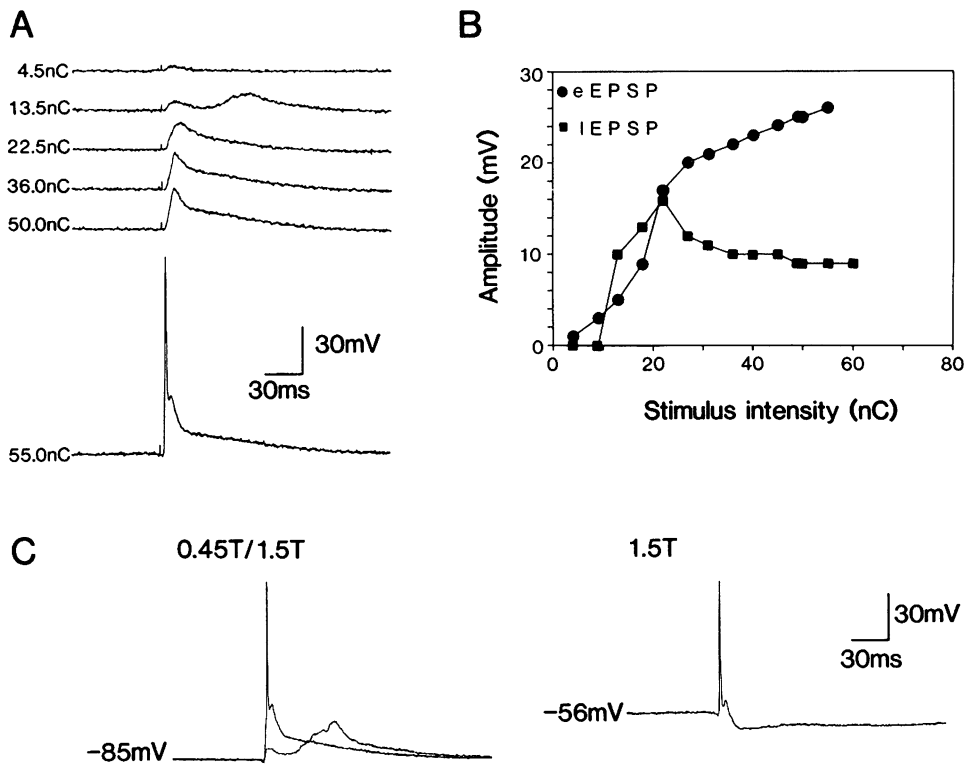

FIG. 4. Stimulus-response relationship of a neocortical neuron. *A*: intracellular recordings of postsynaptic potentials elicited by electrical stimulation of cortical layer IV. The stimulus intensity was gradually increased from the threshold intensity required to evoke an eEPSP (4.5 nC) up to the threshold intensity, T, required to evoke an action potential (55.0 nC). Stimulus frequency, 0.1 Hz; RMP, −83 mV. Note the lEPSP evoked with a stimulus strength of 13.5 nC. *B*: plot of the amplitudes of postsynaptic responses as a function of the stimulus intensity. *Closed circles*: measurement of the amplitude at a time corresponding to the time to peak of the eEPSP. *Closed squares*: measurement of the amplitude at a time corresponding to the time to peak of the lEPSP. Same cell as in *A*. *C*: to illustrate suppression of the lEPSP by IPSPs, synaptic responses evoked by stimulation with intensities of 0.45 and 1.5 T at RMP (−85 mV) were superimposed (*left*). After depolarization to −56 mV, the depolarizing IPSP elicited by stimulation with 1.5 T at RMP was reversed to a hyperpolarizing IPSP (*right*).

high RMP values, the lIPSP was barely evident at RMP. The reversal potential for this lIPSP was −97.9 ± 5.4 mV (n = 5; see also Ref. 16).

Both early and late EPSPs were graded in nature. This was demonstrated by determining input-output curves (Fig. 4*B*), where the amplitudes of the synaptic responses were plotted as a function of the stimulus intensity. When measured at a time corresponding to the time to peak of the eEPSP, response amplitude increased as a function of stimulus strength in all neurons tested (n = 46; Fig. 4*B*, *circles*). Measurements at a time corresponding to the time to peak of the lEPSP yielded an input-output curve that first increased to a maximum value and then declined to a plateau level (Fig. 4*B*, *squares*). This decline coincided with the appearance of the chloride-dependent IPSP. Therefore, beyond the threshold for evoking IPSPs, neither curve rep-

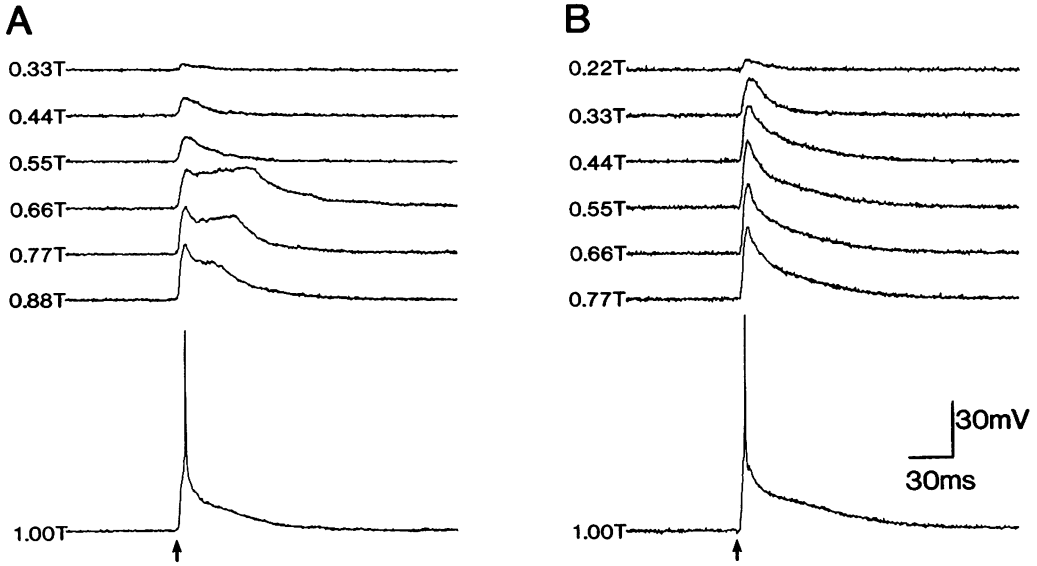

FIG. 5. Variability of the lEPSP. *A*: stimulus-response relationship of a neuron with an RMP of −84 mV. The lEPSP appeared at stimulus intensities between 0.55 and 0.66 T at a very short latency. Note reduction in amplitude of the lEPSP with increasing stimulus intensities. *B*: stimulus-response relationship of another neuron (RMP, −85 mV) in which an lEPSP could not be evoked. Depolarization of the membrane potential revealed the presence of an IPSP following stimulation with 0.33 T.

resents the amplitude of a single synaptic potential, but depicts the net amplitude resulting from the summation of EPSPs and IPSPs.

By choosing appropriate stimulation parameters, the eEPSP could be evoked in isolation in every neuron. This was not the case for the lEPSP. An eEPSP preceded the lEPSP in >95% of neurons showing an lEPSP. The lEPSP was observed in almost every neuron (>90%). The shape of the lEPSP varied from cell to cell (cf. Figs. 4, *A* and *C*, 5, and 11). Due to its longer latency, the lEPSP was usually clearly separated from the eEPSP (see, for example, Fig. 4, *A* and *C*). Furthermore, in a single neuron, the rise time of the late synaptic potential was approximately equal to its decay time, resulting in a symmetrical waveform (e.g., Fig. 4*A*) that was quite distinct from the eEPSP. In some cases, the latency of the lEPSP was short, resulting in a superimposition of the two EPSPs (Figs. 5*A* and 12), which made them difficult to differentiate using a latency criterion, although there were other indications for the presence of the lEPSP [e.g., sensitivity to D-2-amino-5-phosphonovaleric acid (D-2-APV), 47]. However, in a small number of neurons ($n = 6$), all efforts to demonstrate an lEPSP failed. All of these neurons displayed a very low threshold for the elicitation of chloride-dependent IPSPs (0.3–0.4 T; see Fig. 5*B*).

Voltage dependence of the eEPSP/EPSC

Due to the possible involvement of NMDA receptors in the generation of neocortical EPSPs (50), changes in EPSP amplitude during alterations of the membrane potential are of special interest in the cortex and were therefore investigated in detail. The neuron shown in Fig. 6*A* had an RMP of −83 mV. The amplitude of the eEPSP did not increase significantly with depolarization to −66 mV nor did it decrease significantly when hyperpolarized to −96 mV. This behavior is not consistent with an NMDA-mediated synaptic potential. A plot of eEPSP amplitude as a function of membrane potential resulted in a curve with a slope not significantly different from zero, suggesting a very weak underlying synaptic conductance or generation at a site not influenced by somatic current passage. In the neurons tested ($n = 20$), depolarization of the membrane potential by 15–20 mV led to a nonsignificant increase in the amplitude of the eEPSP from 6.6 ± 2.3 to 7.1 ± 2.3 mV. The duration of the eEPSP increased from 47.6 ± 18.2 ms at RMP to 54.7 ± 17.0 ms at membrane potential levels 15–20 mV more positive. This increase in duration was, however, not significant. The only significant change ($P > 0.01$) encountered during membrane potential depolarizations was a prolongation of the time to peak from 8.6 ± 4.2 ms at RMP to 14.2 ± 5.8 ms. This is seen clearly in Fig. 6*B*, where responses at −66 and −83 mV are superimposed.

When the membrane potential was held close to the firing threshold, a stimulus that produced an eEPSP at RMP invariably resulted in the elicitation of an action potential (Fig. 6*C*). These action potentials were followed by a pronounced afterhyperpolarization which decreased the probability of occurrence of a second action potential. However, when the stimulus intensity was increased to values that produced an lEPSP, the conditions for the activation of action potentials changed completely. The now composite EPSP (Fig. 6*D*, −79 mV) was able to evoke action potentials from RMPs well below the firing threshold (Fig. 6*D*, −65 mV). Furthermore, a small afterhyperpolarization

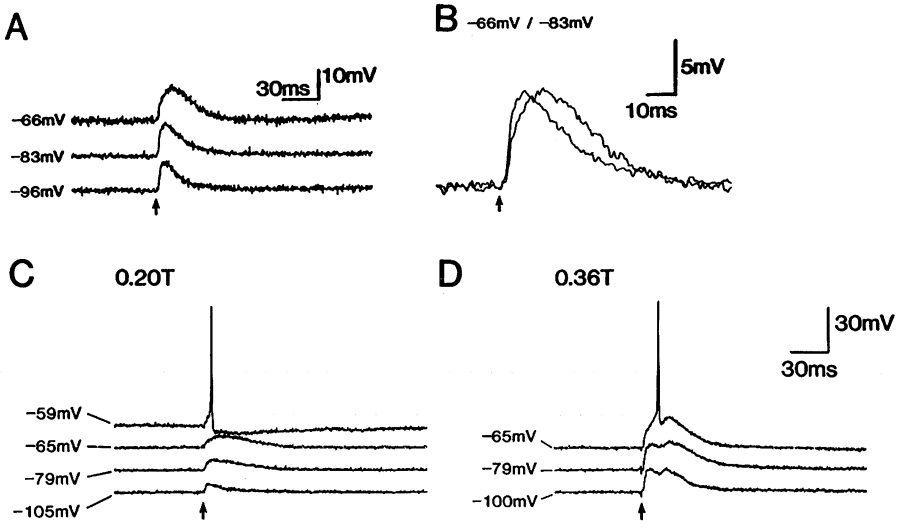

FIG. 6. Voltage dependence of the eEPSP. *A*: eEPSPs evoked at different membrane potentials by stimulation with 12 nC (0.17 T; stimulus frequency, 0.25 Hz; RMP, −83 mV). The membrane potential was changed by injecting depolarizing and hyperpolarizing current pulses of 1-s duration. The stimulus was applied 500 ms after onset of the pulse. Individual current injections were separated by intervals of 10–15 s. Note the decrease in eEPSP amplitude with hyperpolarization. *B*: same neuron as in *A*. The synaptic responses at membrane potentials of −66 and −83 mV, respectively, were enlarged, filtered (500 Hz), and superimposed. In this neuron, there was no increase in amplitude or duration following depolarization, but the time to peak of the eEPSP was increased. *C*: eEPSP produced action potentials only at membrane potential levels close to the firing level (−59 mV; in this neuron, the firing level for direct evoked action potentials was −55 mV; RMP, −79 mV). Note the changes in subthreshold eEPSP amplitude following depolarization and hyperpolarization. *D*: when stimulus intensity was increased from 0.20 to 0.36 T, an lEPSP was evoked. This composite EPSP gave rise to an action potential following depolarization of the membrane potential from −79 to −65 mV.

was followed by a large afterdepolarization (Fig. 6*D*) which increased the probability of activation of a second action potential. Indeed, a slight depolarization of the membrane potential to −63 mV led to the elicitation of a second action potential on top of the peak of the afterdepolarization (not shown).

Since neither the amplitude nor the duration was significantly influenced by depolarization of the membrane potential, the increase in time to peak suggested an alteration in contributions from voltage-dependent currents rather than a change in the underlying synaptic current. To test this hypothesis, single-electrode voltage-clamp measurements were made of the membrane current underlying the eEPSP (eEPSC). In the majority of cells (8 out of 12), an apparent independence of the eEPSC from the membrane potential was observed, as seen under current-clamp conditions. As mentioned in the METHODS section, this unusual finding probably results from nonisopotentiality at the subsynaptic membrane, despite a good voltage clamp of the somatic membrane (i.e., an insufficient space clamp of the neuron). In the remaining four neurons, where apparently better space-clamp conditions were encountered, the amplitude of the eEPSC decreased with depolarization from −80 to −30 mV (Fig. 7). The extrapolated reversal potential for the eEPSP ranged between −5 and +5 mV. Due to the problems associated with inadequate space-clamp conditions, no attempt was made to determine the equilibrium potential of the eEPSP directly by reversing the synaptic potential. From the slope of the relationship between the EPSC amplitude and the membrane potential (Fig. 7*B*), the maximum synaptic conductance was estimated to be 6 nS (determined in a potential range between −80 and −50 mV). It is important to note that there was no detectable change in the eEPSC's time to peak with depolarization (Fig. 7*A*), as would have occurred if changes in the synaptic current were responsible for the prolongation observed in current clamp.

These observations suggest that the eEPSP is probably generated in the distal dendritic region of rat neocortical neurons and that the shape of the eEPSP recorded in the soma of these cells is primarily determined by the nonlinear properties of the somatic membrane and by the cable properties of the dendrites.

Voltage dependence of the lEPSP/lEPSC

The amplitude of the lEPSP increased with hyperpolarization and decreased with depolarization of the membrane potential (Fig. 8, *A* and *B*). This behavior was observed in all neurons tested (n = 35). As already mentioned, the lEPSP was capable of producing action potentials when evoked at membrane potentials 10–20 mV negative to the firing threshold for directly evoked action potentials (about −50 mV; see Figs. 6*D* and 8*A*).

In contrast to the eEPSP, the lEPSP could be easily influenced by somatic current passage and the voltage-clamp analysis employed (Fig. 8*C*; n = 8). Plots of the lEPSC amplitude as a function of the holding potential yielded curves that confirmed the observations made under current-clamp conditions: the amplitude of the lEPSC increased with hyperpolarization and decreased with depolarization (Fig. 8*E*). The extrapolated reversal potential of the lEPSC ranged between 0 and +5 mV. The conductance that produced the lEPSP was 6–10 nS, as estimated from the slope of the relationship between EPSC amplitude and membrane potential (Fig. 8*E*).

That the lEPSP was easily influenced by current injection into the soma, together with the finding that the lEPSP showed the same voltage dependence as the lEPSC, suggests that the lEPSP is generated at a site readily influenced

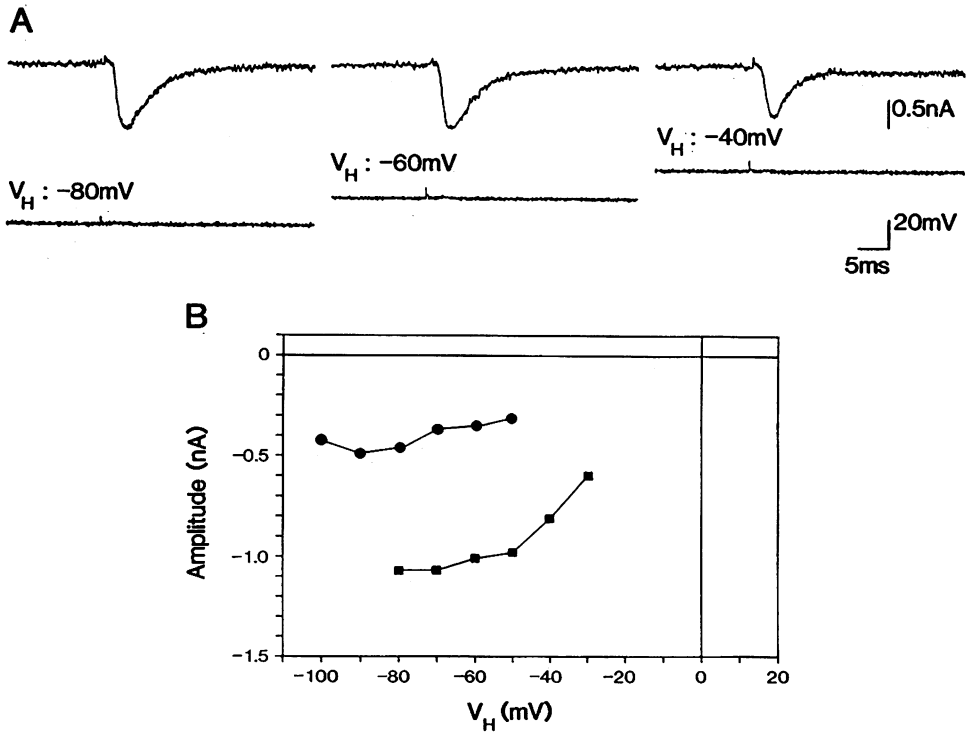

FIG. 7. Voltage dependence of the eEPSC. *A*: single-electrode voltage-clamp recordings of an eEPSC activated by stimulation with 4.5 nC (0.21 T; stimulus frequency, 0.25 Hz; RMP, −82 mV). The holding potential (V_H) was decreased from −80 to −30 mV in increments of 10 mV (see *B, squares*). Each trace depicted represents the average of 5 single measurements. *B*: plot of eEPSC amplitude as a function of V_H. The *circles* and *squares* represent measurements from 2 different neurons.

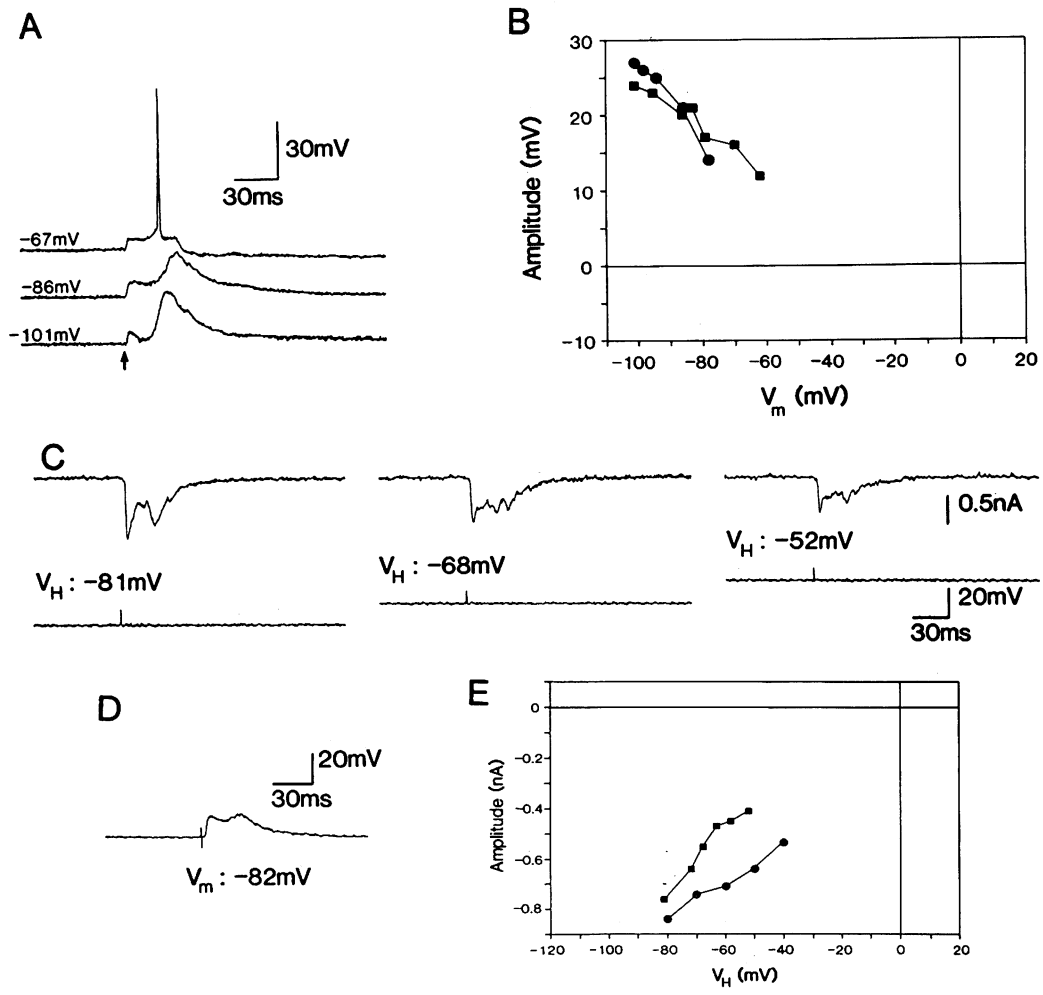

FIG. 8. Voltage dependence of the lEPSP. *A*: postsynaptic responses recorded at different membrane potentials following electrical stimulation with 10 nC (0.35 T; stimulus frequency, 0.1 Hz; RMP, −86 mV). At RMP, the stimulus evoked an eEPSP and an lEPSP. The membrane potential was changed using the method described in Fig. 6. Note the action potential elicited by the lEPSP at a membrane potential of −67 mV. *B*: plot of lEPSP amplitude as a function of membrane potential. The *circles* and *squares* represent measurements from 2 different neurons. *C*: voltage dependence of the lEPSC. Voltage-clamp recordings of an lEPSC at different holding potentials (V_H) (RMP, −82 mV). The synaptic current was evoked by electrical stimulation with 10.5 nC (0.41 T; stimulus frequency, 0.1 Hz). Since the lEPSC was superimposed on the eEPSC, both the early and the late peak amplitudes of the synaptic current decreased with depolarization. *D*: current-clamp recording of the lEPSP corresponding to the lEPSC detected at a V_H of −81 mV. *E*: plot of lEPSC amplitude as a function of V_H. The *squares* and *circles* represent measurements from 2 different neurons.

by somatic current passage, i.e., within the proximal dendritic region or on the soma of rat neocortical neurons.

Frequency-dependent short-term depression of the lEPSP

The lEPSP was not able to follow stimulation at frequencies ≥ 0.5 Hz. Figure 9 shows a neuron in which the amplitudes of the eEPSP and lEPSP were measured as a function of stimulus number at different stimulus frequencies. A stimulus with an intensity of 10 nC elicited an eEPSP (Fig. 9*A*) whose amplitude was not influenced by a change in stimulus frequency from 0.1 (Fig. 9*A*, *left*, and 9*C*, *circles*) to 1.0 Hz (Fig. 9*A*, *right*, and 9*C*, *squares*). When stimulus strength was increased to 12.5 nC, the neuron responded with an eEPSP followed by an lEPSP. At a stimulus frequency of 0.1 Hz, there was no detectable attenuation of the amplitude of the lEPSP (Fig. 9*B*, *left* and 9*D*, *triangles*). However, at a stimulus frequency of 1.0 Hz, only the first stimulus successfully elicited an lEPSP; the following nine stimuli evoked only eEPSPs (Fig. 9*B*, *right*, and 9*D*, *hexagons*). The amplitude of the eEPSP produced by a stimulus intensity of 12.5 nC remained unaltered (Fig. 9, *B* and *D*, *circles* and *squares*). The frequency-dependent depression of the lEPSP reversed very rapidly. After the last stimulus at 1.0 Hz, the frequency was reset to 0.1 Hz, and the first stimulus elicited a fully recovered lEPSP. Thus full recovery occurred within 10 s.

Long-term potentiation of the lEPSP

A second type of frequency-dependent change in the lEPSP was a sustained increase in amplitude following high-frequency stimulation (HFS). The stimulation pattern consisted of 1–4 trains of 100 Hz delivered at intervals of 5

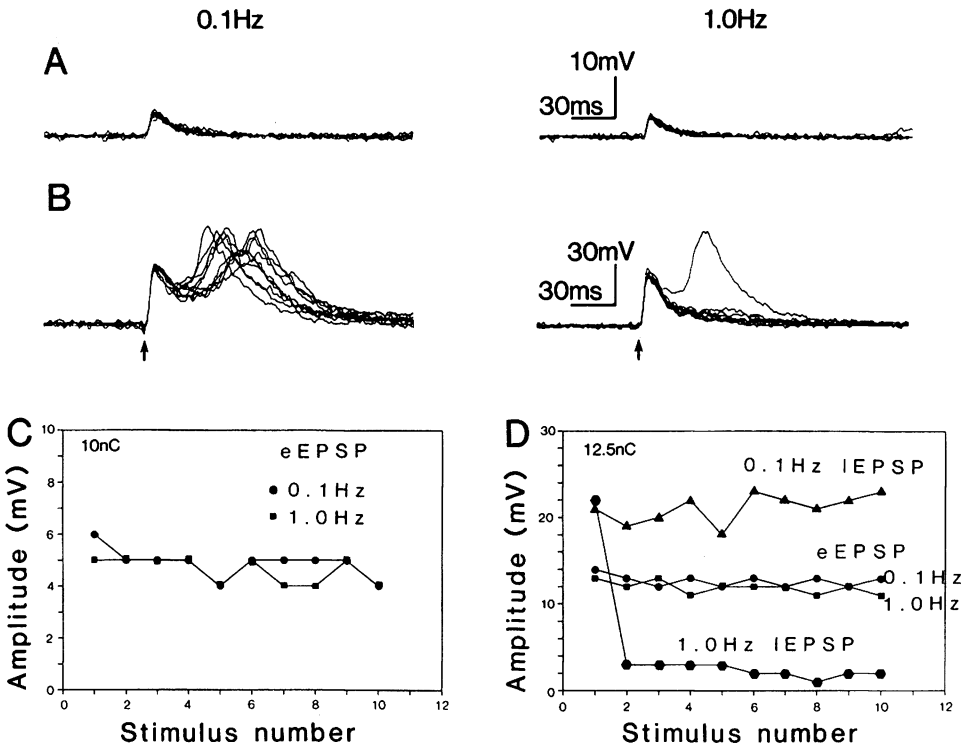

FIG. 9. Frequency-dependent depression of the IEPSP. *A*: eEPSPs evoked by 10 consecutive stimuli at a frequency of 0.1 Hz (*left*) and 1.0 Hz (*right*). Stimulus intensity, 10 nC; RMP, −81 mV. Both panels depict the superimposed synaptic responses. *B*: eEPSPs and IEPSPs elicited by 10 consecutive stimuli at a frequency of 0.1 Hz (*left*) and 1.0 Hz (*right*). Stimulus intensity, 12.5 nC; same neuron as in *A*. Voltage traces in *A* and *B* were filtered at 500 Hz. *C*: plot of eEPSP amplitude as a function of stimulus number. *Circles*: stimulus frequency, 0.1 Hz. *Squares*: stimulus frequency, 1.0 Hz. Stimulus intensity, 10 nC (see *A*). *D*: plot of eEPSP amplitude and IEPSP amplitude as a function of stimulus number. *Circles*: peak amplitude of the eEPSP at 0.1 Hz. *Squares*: peak amplitude of the eEPSP at 1.0 Hz. *Triangles*: peak amplitude of the IEPSP at 0.1 Hz. *Hexagons*: peak amplitude of the IEPSP at 1.0 Hz. Stimulus intensity, 12.5 nC (see *B*).

s (see Ref. 22) using a stimulus strength equal to 0.5–1.0 times the intensity necessary to evoke an eEPSP. The effect of such tetanic stimulation is shown in Fig. 10*A*. Under control conditions, stimulation evoked only an eEPSP. After HFS, there was an apparent increase in the eEPSP and the appearance of an IEPSP. The time course of LTP induction in rat neocortical neurons is shown in Fig. 10*B*. The action of HFS on the IEPSP started within 7–15 min

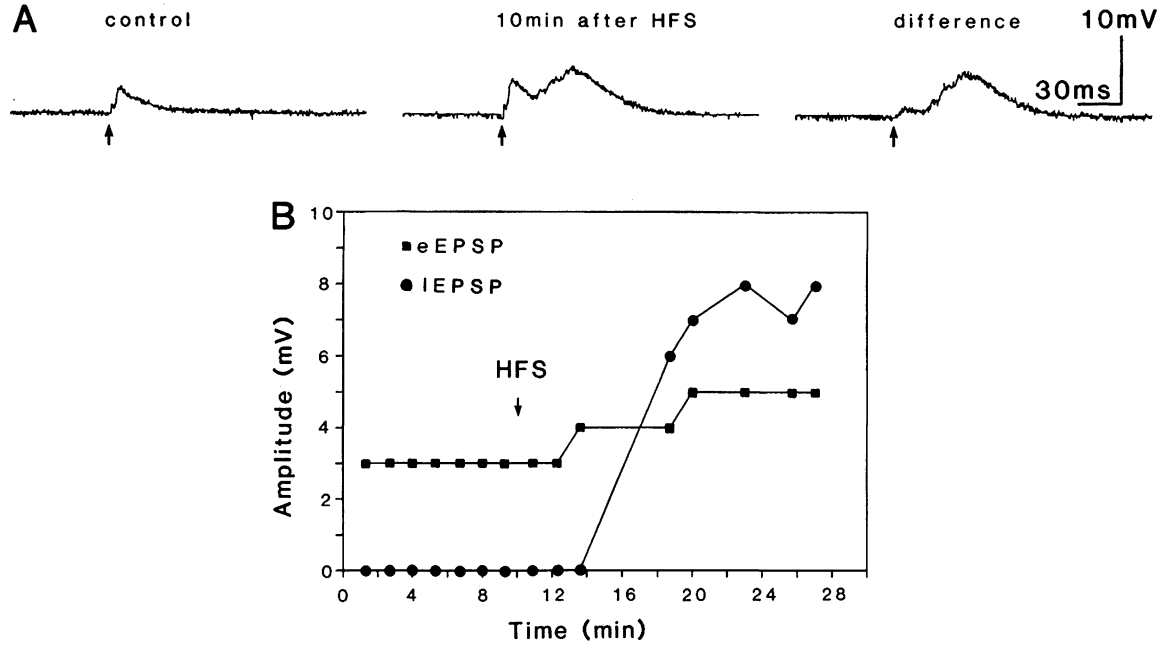

FIG. 10. Long-term potentiation (LTP) of the IEPSP induced by HFS. *A*: intracellular recordings of excitatory postsynaptic potentials activated by stimulation with 7.5 nC (0.24 T; stimulus frequency, 0.1 Hz; RMP, −84 mV) before (control) and 10 min after HFS (4 trains at 100 Hz for 1 s, delivered at 5-s intervals; stimulus intensity = 3.8 nC or 0.5 times the threshold intensity necessary to evoke an eEPSP). The rightmost trace was obtained by digital subtraction of the control response from the potentiated response. Each trace represents an average of 10 consecutive single measurements. *B*: graphic depiction of the time course of LTP development in neocortical neurons (same neuron as in *A*). *Circles*: peak amplitude of the IEPSP. *Squares*: peak amplitude of the eEPSP. The enhancement of the eEPSP amplitude is due to the superimposition of the eEPSP and the IEPSP. Each point in the diagram corresponds to the average of 10 consecutive single measurements.

and reached a constant level after 15–25 min. In 12 out of 14 neurons, the HFS-induced changes persisted for the duration of the observation period (up to 5 h). In two neurons, the increased amplitude of the lEPSP declined to control levels 45 and 60 min, respectively, following HFS.

In most cells, the eEPSP was not influenced by HFS. In some instances, there was an apparent increase in its amplitude following tetanic stimulation, probably due to a superimposition of the enhanced lEPSP on the eEPSP (Fig. 11*A*). However, in a few cells (n = 3), a true decrease in eEPSP threshold intensity was observed (Fig. 11, *A* and *B*), indicating an enhancement of the efficacy of the synaptic transmission underlying the eEPSP.

The effects of HFS on the lEPSP were detectable only in a limited range of test stimulus intensities. Figure 11 shows the postsynaptic responses of a neuron to stimulation with different stimulus strengths before (Fig. 11*A*) and after (Fig. 11*B*) HFS. A stimulus with an intensity of 3 nC, which was ineffective before, produced an eEPSP following HFS. The synaptic responses evoked by intensities between 9 and 21 nC were enhanced after HFS. However, there was no significant difference between the potential sequences elicited by threshold intensity (24 nC) before and after HFS. The reason for this phenomenon was the appearance of chloride- and potassium-dependent IPSPs at higher stimulus strengths. The conductance underlying these inhibitory potentials was not attenuated by HFS and was therefore strong enough to shunt even potentiated lEPSPs.

In 6 neurons in which the lEPSP was enhanced by HFS, the membrane potential, I-V relation, and discharge behavior evoked by direct current injection were determined before and after the tetanus. No changes were observed.

DISCUSSION

The experiments described here provide evidence for the existence of two distinct EPSPs in layer II/III neurons of rat frontal cortex. The EPSPs differ in amplitude, time to peak, duration, voltage dependence of amplitude, and sensitivity to changes in stimulus frequency. These EPSPs were recorded from neocortical neurons whose electrophysiological properties were similar to those of identified regular-spiking pyramidal cells (29, 48). On the basis of these similarities, we assume that the majority of the neurons recorded in the rat medial precentral cortex were layer II/III pyramidal cells.

The EPSPs were evoked by electrical stimulation of an area corresponding to layer IV of the frontal cortex (~1,000 μm below the pial surface). This area was chosen because it is known to be the relay station of thalamocortical afferent input (32). In the rat neocortex, ~80% of thalamic fibers form asymmetrical, i.e., presumably excitatory, synapses with dendritic spines of layer IV neurons (52). The layer IV neurons send their axons to cells in other cortical layers, including pyramidal cells of layer II/III. These pathways are either monosynaptic or involve one or

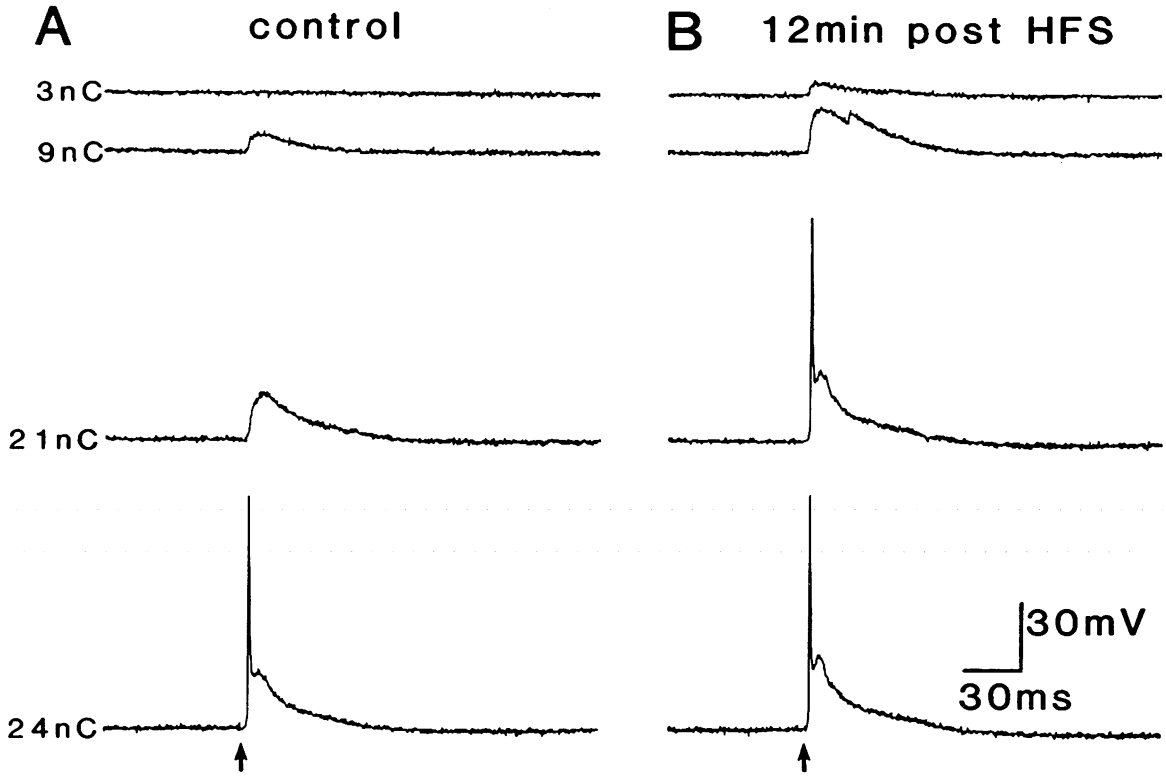

FIG. 11. Stimulus-response relationship of neocortical neurons before and after HFS. *A*: postsynaptic responses to electrical stimulation with increasing intensities before HFS (control) stimulus frequency, 0.1 Hz; RMP: −83 mV). *B*: postsynaptic responses to stimulation with the same intensities 12 min following HFS (12 min post HFS) (RMP, −83 mV). HFS, 4 trains at 100 Hz for 1 s; intervals, 5 s; stimulus intensity, 3 nC. Note the almost identical postsynaptic responses to stimulation with 24 nC before and after HFS. Note also that the stimulus intensity used to induce LTP (3 nC) did not evoke a detectable response under control conditions.

more interneurons (38). It is important to note that only 30% of the fibers establishing asymmetrical synapses in the neocortex originate from neurons extrinsic to the cortex. The other 70% comprise axons from intrinsic neocortical neurons that form local excitatory circuits within the neocortex (32).

Because of the complex interconnections between neocortical neurons (32), a similar, complex pattern of postsynaptic responses of layer II/III neurons to electrical stimulation of neuronal elements in layer IV would be expected. The markedly stereotyped response pattern observed in the present study (see Figs. 4 and 5) does not seem to confirm these expectations. However, a uniform stimulus-response pattern does not exclude the existence of a complicated network; rather, it demonstrates that the experimental conditions chosen (e.g., slicing procedure, arrangement of recording and stimulating electrodes) allowed investigation of a stimulus-response relationship that was quite reproducible among the population of neurons examined.

Properties of eEPSP

Electrical stimulation with very low intensities evoked a short-latency EPSP (eEPSP) that produced action potentials when elicited at membrane potentials close to the firing threshold of the neuron. The eEPSP was the only synaptic potential that could be elicited virtually in isolation, i.e., not overlapped by other synaptic potentials. With hyperpolarization of the membrane potential, the amplitude of the eEPSP decreased. After depolarization to subthreshold levels, a nonsignificant increase in the amplitude of the eEPSP was observed. This voltage dependence of the eEPSP amplitude was quite unusual compared with EPSPs described in other regions of the brain (see Refs. 8, 12, 14, 26). Assuming a conventional generating mechanism with an equilibrium potential (E_{eEPSP}) close to 0 mV (12), the eEPSP should increase with hyperpolarization and decrease with depolarization. There are two possible explanations for the uncommon behavior of the eEPSPs amplitude following changes in the membrane potential: *1*) the ionic conductance producing the eEPSP (g_{eEPSP}) is voltage dependent, i.e., it increases with depolarization and decreases with hyperpolarization. If g_{eEPSP} is strong enough to dominate the total membrane conductance, at least transiently, both the synaptic current and synaptic potential will decrease with hyperpolarization and increase with a reduction in the membrane potential. *2*) The g_{eEPSP} is independent of the membrane potential but is connected in parallel to strong membrane conductances displaying inward rectification in both the hyperpolarizing and depolarizing directions. Thus the shape of the resulting eEPSP, at a given membrane potential, will depend on the magnitude of g_{eEPSP} and on the properties of the predominant conductance at this potential. However, the eEPSC, measured under voltage-clamp conditions, will show a linear relationship to the membrane potential, unless strong noninactivating membrane conductances are in parallel.

The first explanation was used by Thomson (50) to describe the mechanism of an EPSP recorded in rat neocortical neurons in vitro. In that study, the amplitude of the white matter evoked EPSP decreased with hyperpolarization and increased with depolarization, similar to the amplitude of the eEPSP. This voltage dependence resembled the well-known changes in the amplitude of an NMDA-induced depolarization following shifts in the membrane potential (for review, see Ref. 28). Since the EPSPs amplitude was found to be voltage independent following a reduction in the extracellular magnesium concentration and since the selective NMDA antagonist D-2-APV, applied by iontophoresis, was able to block the EPSP, it was concluded that this EPSP is mediated by the activation of synaptic NMDA receptors (50).

Although these interpretations provide a convincing explanation of the behavior of the EPSP observed by Thomson (50), some electrophysiological properties of the eEPSP recorded in the present study are not in accord with the hypothesis of an NMDA-mediated synaptic potential, despite similarities in voltage dependence between the EPSP described by Thomson and the eEPSP we described. First, the slight increase in eEPSP amplitude we observed with depolarization was not statistically significant. In fact, repeated depolarizations to the same potential level revealed a large variability in the eEPSP amplitude. NMDA responses in cortical neurons are consistently more voltage dependent (47). Second, in a majority of neurons, the current underlying the eEPSP (eEPSC) was apparently independent of the membrane potential. In no cell did the eEPSC increase with depolarization. Third, following depolarization of the membrane potential, there was a significant increase in the time to peak of the eEPSP, but no corresponding increase in the time to peak of the eEPSC, indicating that other factors, in addition to g_{eEPSP}, determined the shape of the eEPSP.

On the basis of our observations, we propose the following hypothesis to account for the behavior of the eEPSP we recorded: the eEPSP was generated at synapses remote from the area of the neuron that could be effectively controlled by the microelectrode presumably lodged in the soma. The effectively controlled area probably comprised either the soma and parts of the proximal dendrites or only the soma or parts of it (17) (for convenience, this area will be called the somatic site). The eEPSP was conducted from its site of origin to the somatic site via the distal and proximal dendrites. Consequently, the eEPSP detected at somatic sites did not represent the "real" synaptic potential, since both the time course and amplitude of the "real" eEPSP were altered by the cable properties of the dendrites (37). Accordingly, the eEPSC recorded from the soma was not the synaptic current "injected" by the synapse, but the current necessary to prevent voltage deviations at the somatic membrane during the synaptic response. Therefore, neither the synaptic current nor the synaptic potential recorded at somatic sites could be used to determine the properties of g_{eEPSP}. Since the site of origin was remote from the somatic area, current injections into the soma would reliably and reproducibly change the driving force of the eEPSC (18), resulting in an apparent independence of the synaptic current from the membrane potential. Moreover, the shape of the eEPSP recorded at somatic sites was determined by the nonlinearities of the *I-V* relationship present in neocortical neurons (see Fig. 2). When the membrane potential was hyperpolarized, the R_N decreased due to anomalous rectification (see Figs. 2 and 3; see also Refs. 9, 39–41, 48, 50). Simultaneously, the amplitude of

the eEPSP was reduced (see also Ref. 30). Upon depolarization, an apparent increase in R_N, produced by activation of voltage-dependent sodium and calcium conductances (9, 13, 40, 41, 48), was observed. This apparent enhancement in R_N was sufficient to explain the slight increase in the amplitude of the eEPSP (see also Ref. 40). The inactivation with depolarization of a low-voltage activated calcium conductance (13, 48) might also account for the increase in time to peak of the eEPSP following depolarization.

From this hypothesis, three predictions can be made: *1*) at every membrane potential, the eEPSP should be insensitive to the selective NMDA antagonist D-2-APV; *2*) reductions in the extracellular magnesium concentration should not affect the eEPSP's voltage dependence; and *3*) following drug-induced changes in the neuron's *I-V* relationship, there must be parallel changes in the relationship between the shape of the eEPSP and the membrane potential. These predictions were investigated, and the results are presented in the following paper (47).

Mechanisms for lEPSP generation

A delayed depolarizing potential (lEPSP) followed the eEPSP when stimulus intensities were increased. The lEPSP was graded in nature and showed large latency fluctuations. In contrast to the eEPSP, the amplitudes of both the lEPSP and the lEPSC could be readily influenced by current injection into the soma. The amplitudes decreased with depolarization and increased with hyperpolarization. The effects of current injection on the amplitude of the lEPSP and the lEPSC, respectively, were almost identical, suggesting that the lEPSP is generated at synapses located at or close to somatic sites that were sufficiently voltage- and space-clamped. However, the degree to which the somatically recorded lEPSC waveform reflects the true subsynaptic current is not known, since the exact location of the synapses generating the lEPSP is not known.

The lEPSP displayed four unique features: *1*) the lEPSP was capable of producing action potentials when evoked at membrane potentials 10–20 mV more negative than the normal firing level. In contrast, a pure eEPSP evoked a spike only when the membrane potential was close to the action potential threshold. This property of the lEPSP allows the neurons to produce action potentials phasically in response to activation of a pathway producing lEPSPs, even if the RMP is far from the firing level for directly evoked spikes. *2*) When the stimulus strength reached the threshold intensity for the activation of IPSPs, the lEPSP disappeared (Fig. 4). We attribute this phenomenon to a shunt of the lEPSP by the large conductance increase associated with IPSPs. The consequence was that the lEPSP could be observed only in a limited range of stimulus intensities. Connors et al. (9) described a similar delayed depolarizing potential in guinea-pig neocortical neurons which disappeared with increasing stimulus intensities, suggesting that the lEPSP is a common synaptic potential in neocortical neurons. *3*) The lEPSP was not able to follow stimulus frequencies > 0.5 Hz. This frequency-dependent short-term depression suggests that the lEPSP was generated by disynaptic or polysynaptic pathways (5). The fast recovery of the lEPSP and our results with iontophoresis of NMDA (47) excludes the alternative possibility that the receptors activated by the endogenously released transmitter mediating the lEPSP were desensitized. *4*) HFS led to a sustained increase in the amplitude of the lEPSP. The stimulus pattern used to evoke this response has been shown to induce LTP of field potentials recorded in the neocortex (25). The ability of the neocortex to display enhancement in the efficiency of excitatory synaptic transmission, resembling LTP in hippocampal neurons following tetanic stimulation, has been reported by several groups (2–4, 6, 7, 23–25). However, the present study is the first report of a selective potentiation of a polysynaptic EPSP. Since the electrophysiological properties of the neurons remained unaltered following HFS, it is justified to assume that the LTP observed in neocortical neurons is produced by a synaptic mechanism. In every neuron in which LTP was successfully induced (14 out of 16), the lEPSP could be evoked before HFS by using stimulus intensities subthreshold for the activation of IPSPs. An important observation of the present study is that the IPSPs did not lose their ability to block the lEPSP following induction of LTP by HFS. Consequently, the effects of HFS, i.e., the enhanced amplitude of the lEPSP, could be detected only at stimulus intensities subthreshold for the activation of IPSPs. The neuronal circuitry underlying this mechanism may represent an effective instrument for controlling the transmission of information contained in EPSPs that were potentiated by repetitive excitatory synaptic input. LTP in neocortical neurons could be induced using stimulus intensities that did not evoke a detectable postsynaptic response in the neuron recorded, suggesting that the primary process leading to LTP did not occur in that neuron but in excitatory local circuit neurons (47).

This work was supported by National Institute of Neurological and Communicative Disorders and Stroke Grants NS-22373 and NS-18145, by Deutsche Forschungsgemeinschaft Grant Su 104/1-1, and by a Fellowship Award from the Max Kade Foundation to B. Sutor.

Present address of B. Sutor: Physiologisches Institut der Universität, Pettenkoferstrasse 12, 8000 München 2, FRG.

Address for reprint requests: J. Hablitz, Neurobiology Research Center, Department of Physiology and Biophysics, University of Alabama at Birmingham, Birmingham, AL 35294.

Received 21 July 1988; accepted in final form 21 October 1988.

REFERENCES

1. ARMSTRONG, D. M. Synaptic excitation and inhibition of Betz cells by antidromic pyramidal volleys. *J. Physiol. Lond.* 178: 37–38P, 1965.
2. ARTOLA, A. AND SINGER, W. Long-term potentiation and NMDA receptors in rat visual cortex. *Nature Lond.* 330: 649–652, 1987.
3. BARANYI, A. AND FEHER, O. Conditioned changes of synaptic transmission in the motor cortex of the cat. *Exp. Brain Res.* 33: 283–298, 1978.
4. BARANYI, A. AND SZENTE, M. Long-lasting potentiation of synaptic transmission requires postsynaptic modification in the neocortex. *Brain Res.* 423: 378–384, 1987.
5. BERRY, M. S. AND PENTREATH, V. W. Criteria for distinguishing between monosynaptic and polysynaptic transmission. *Brain Res.* 105: 1–20, 1976.
6. BINDMAN, L. J., LIPPOLD, O. C. J., AND MILNE, A. R. Prolonged changes in excitability of pyramidal tract neurones in the cat: a postsynaptic mechanism. *J. Physiol. Lond.* 286: 457–477, 1979.
7. BINDMAN, L. J., MEYER, T., AND POCKETT, S. Long-term potentiation in rat neocortical neurones in slices, produced by repetitive pairing of an afferent volley with intracellular depolarizing current. *J. Physiol. Lond.* 386: 90P, 1987.
8. BROWN, T. H. AND JOHNSTON, D. Voltage-clamp analysis of mossy fiber synaptic input to hippocampal neurons. *J. Neurophysiol.* 50: 487–507, 1983.

9. CONNORS, B. W., GUTNICK, M. J., AND PRINCE, D. A. Electrophysiological properties of neocortical neurons in vitro. *J. Neurophysiol.* 48: 1302–1320, 1982.
10. DEMPSEY, E. W. AND MORISON, R. S. The electrical activity of a thalamocortical relay system. *Am. J. Physiol.* 138: 283–296, 1942.
11. DEMPSEY, E. W. AND MORISON, R. S. The mechanism of thalamocortical augmentation and repetition. *Am. J. Physiol.* 138: 297–308, 1942.
12. ECCLES, J. C. *The Physiology of Synapses.* Berlin: Springer-Verlag, 1964.
13. FRIEDMAN, A. AND GUTNICK, M. J. Low-threshold calcium electrogenesis in neocortical neurons. *Neurosci. Lett.* 81: 117–122, 1987.
14. HABLITZ, J. J. AND LANGMOEN, I. A. Excitation of hippocampal pyramidal cells by glutamate in the guinea-pig and rat. *J. Physiol. Lond.* 325: 317–331, 1982.
15. HOWE, J. R., SUTOR, B., AND ZIEGLGÄNSBERGER, W. Baclofen reduces post-synaptic potentials of rat cortical neurons by an action other than its hyperpolarizing action. *J. Physiol. Lond.* 384: 539–569, 1987.
16. HOWE, J. R., SUTOR, B., AND ZIEGLGÄNSBERGER, W. Characteristics of long-duration inhibitory postsynaptic potentials in rat neocortical neurons in vitro. *Cell. Mol. Neurobiol.* 7: 1–18, 1987.
17. JACK, J. J. B., NOBLE, D., AND TSIEN, R. W. *Electric Current Flow in Excitable Cells.* Oxford, UK: Clarendon, 1983.
18. JOHNSTON, D. AND BROWN, T. H. Interpretation of voltage-clamp measurements in hippocampal neurons. *J. Neurophysiol.* 50: 464–486, 1983.
19. KANG, Y., ENDO, K., AND ARAKI, T. Excitatory synaptic actions between pairs of neighboring pyramidal tract cells in the motor cortex. *J. Neurophysiol.* 59: 636–647, 1988.
20. KLEE, M. R. Different effects on the membrane potential of motor cortex units after thalamic and reticular stimulation. In: *The Thalamus,* edited by D. P. Purpura and M. D. Yahr. New York: Columbia Univ. Press, 1966, p. 287–322.
21. KLEE, M. R. AND LUX, H. D. Intracellulaere Untersuchungen über den Einfluss hemmender Potentiale im motorischen Cortex. II. Die Wirkung elektrischer Reizung des Nucleus caudatus. *Arch. Psychiatr. Nervenkr.* 203: 667–689, 1962.
22. KLEE, M. R. AND OFFENLOCH, K. Postsynaptic potentials and spike patterns during augmenting responses in cat motor cortex. *Science Wash. DC* 143: 488–489, 1964.
23. KOMATSU, Y., FUJII, K., MAEDA, J., SAKAGUCHI, H., AND TOYAMA, K. Long-term potentiation of synaptic transmission in kitten visual cortex. *J. Neurophysiol.* 59: 124–141, 1988.
24. KOMATSU, Y., TOYAMA, K., MAEDA, J., AND SAKAGUCHI, H. Long-term potentiation investigated in a slice preparation of striate cortex of young kittens. *Neurosci. Lett.* 26: 269–274, 1981.
25. LEE, K. Sustained enhancement of evoked potentials following brief, high-frequency stimulation of the cerebral cortex in vitro. *Brain Res.* 239: 617–623, 1982.
26. LLINAS, R. AND SUGIMORI, M. Electrophysiological properties of in vitro Purkinje cell somata in mammalian cerebellar slices. *J. Physiol. Lond.* 305: 171–195, 1980.
27. LUX, H. D. AND KLEE, M. R. Intracellulaere Untersuchungen über den Einfluss hemmender Potentiale im motorischen Cortex. I. Die Wirkung elektrischer Reizung unspezifischer Thalamuskerne. *Arch. Psychiatr. Nervenkr.* 203: 648–666, 1962.
28. MAYER, M. L. AND WESTBROOK, G. L. The physiology of excitatory amino acids in the vertebrate central nervous system. *Prog. Neurobiol.* 28: 197–276, 1986.
29. MCCORMICK, D. A., CONNORS, B. W., LIGHTHALL, J. W., AND PRINCE, D. A. Comparative electrophysiology of pyramidal and sparsely spiny stellate neurons of the neocortex. *J. Neurophysiol.* 54: 782–806, 1985.
30. NELSON, P. G. AND FRANK, K. Anomalous rectification in cat spinal motoneurons and effect of polarizing currents on excitatory postsynaptic potential. *J. Neurophysiol.* 30: 1097–1113, 1967.
31. OSHIMA, T. Studies of pyramidal tract cells. In: *Basic Mechanisms of the Epilepsies,* edited by H. H. Jasper, A. A. Ward, Jr., and A. Pope. Boston, MA: Little, Brown, 1969, p. 253–261.
32. PETERS, A. Synaptic specificity in the cerebral cortex. In: *Synaptic Function,* edited by G. M. Edelman, W. E. Gall, and W. M. Cowan. New York: Wiley, 1987, p. 373–397.
33. PHILLIPS, C. G. Intracellular records from Betz cells in the cat. *Q. J. Exp. Physiol.* 41: 58–69, 1956.
34. POLDER, H.-R. Entwurf und Aufbau eines Gerätes zur Untersuchung der Membranleitfaehigkeit von Nervenzellen und deren Nichtlinearitaet nach der potentiostatischen Methode (Voltage-clamp-Methode) mittels einer Mikroelektrode. Diplomarbeit, Fachbereich Elektrotechnik, TU München, 1984.
35. PURPURA, D. P. AND SHOFER, R. J. Cortical intracellular potentials during augmenting and recruiting responses. I. Effects of injected hyperpolarizing currents on evoked membrane potential changes. *J. Neurophysiol.* 27: 117–132, 1964.
36. PURPURA, D. P., SHOFER, R. J., AND MUSGRAVE, F. S. Cortical intracellular potentials during augmenting and recruiting responses. II. Patterns of synaptic activities in pyramidal and nonpyramidal tract neurons. *J. Neurophysiol.* 27: 133–151, 1964.
37. RALL, W. Core conductor theory and cable properties of neurons. In: *Handbook of Physiology. The Nervous System.* Bethesda, MD: Am. Physiol. Soc. 1977, sect. 1, vol. I, part 1, p. 39–97.
38. SCHMITT, F. O., WORDEN, F. G., ADELMAN, G., DENNIS, S. G. *The Organization of the Cerebral Cortex.* Cambridge, MA: MIT Press, 1981.
39. SPAIN, W. J., SCHWINDT, P. C., AND CRILL, W. E. Anomalous rectification in neurons from the cat sensorimotor cortex in vitro. *J. Neurophysiol.* 57: 1555–1576, 1987.
40. STAFSTROM, C. E., SCHWINDT, P. C., CHUBB, M. C., AND CRILL, W. E. Properties of persistent sodium conductance and calcium conductance in layer V neurons from cat sensorimotor cortex in vitro. *J. Neurophysiol.* 53: 153–170, 1985.
41. STAFSTROM, C. E., SCHWINDT, P. C., FLATMAN, J. A., AND CRILL, W. E. Properties of subthreshold response and action potential recorded in layer V neurons from cat sensorimotor cortex in vitro. *J. Neurophysiol.* 52: 244–263, 1984.
42. STEFANIS, C. AND JASPER, H. H. Intracellular microelectrode studies of antidromic responses in cortical pyramidal tract neurons. *J. Neurophysiol.* 27: 828–854, 1964.
43. STEFANIS, C. AND JASPER, H. H. Recurrent collateral inhibition in pyramidal tract neurons. *J. Neurophysiol.* 27: 855–877, 1964.
44. SUTOR, B. *Nachweis eines GABA-vermittelten, inhibitorischen postsynaptischen Potentials in Neuronen des Neokortex der Ratte (Rattus norvegicus)* (PhD thesis). Nürnberg, FRG: University of Erlangen, 1986.
45. SUTOR, B. AND HABLITZ, J. J. Properties of subthreshold EPSPs in rat neocortical neurons. *Soc. Neurosci. Abstr.* 13: 156, 1987.
46. SUTOR, B. AND HABLITZ, J. J. Electrophysiological properties of excitatory postsynaptic potentials in rat neocortical neurons in vitro. *Pfluegers Arch.* 411, *Suppl.* I: R153, 1988.
47. SUTOR, B. AND HABLITZ, J. J. Excitatory postsynaptic potentials in rat neocortical neurons in vitro. II. Involvement of *N*-methyl-D-aspartate receptors in the generation of EPSPs. *J. Neurophysiol.* 61: 621–634, 1989.
48. SUTOR, B. AND ZIEGLGÄNSBERGER, W. A low-voltage activated, transient calcium current is responsible for the time-dependent depolarizing inward rectification of rat neocortical neurons in vitro. *Pfluegers Arch.* 410: 102–111, 1987.
49. TAKAHASHI, K., KUBOTA, K., AND UNO, M. Recurrent facilitation in cat pyramidal tract cells. *J. Neurophysiol.* 30: 22–34, 1967.
50. THOMSON, A. M. A magnesium-sensitive post-synaptic potential in rat cerebral cortex resembles neuronal responses to *N*-methylaspartate. *J. Physiol. Lond.* 370: 531–549, 1986.
51. TSUKAHARA, N., FULLER, D. R. G., AND BROOKS, V. B. Collateral pyramidal influences on the cortico-rubrospinal system. *J. Neurophysiol.* 31: 467–484, 1968.
52. VAUGHAN, D. W. AND PETERS, A. Proliferation of thalamic afferents in cerebral cortex altered by callosal deafferentiation. *J. Neurocytol.* 14: 705–716, 1985.
53. VOGT, B. A. AND GORMAN, A. L. F. Responses of cortical neurons to stimulation of corpus callosum in vitro. *J. Neurophysiol.* 48: 1257–1273, 1982.
54. WEISS, D. S. AND HABLITZ, J. J. Interaction of penicillin and pentobarbital with inhibitory synaptic mechanisms in neocortex. *Cell. Mol. Neurobiol.* 4: 301–317, 1984.